Study of the Response Surface in the Photocatalytic Degradation of Acetaminophen Using TiO₂

Adriana Marizcal-Barba [1], Jorge Alberto Sanchez-Burgos [2], Victor Zamora-Gasga [2] and Alejandro Perez Larios [1,*]

[1] Materials, Water and Energy Research Laboratory, Department of Engineering, Los Altos University Center, University of Guadalajara, Tepatitlán de Morelos 47600, Mexico; adriana.marizcal7736@alumnos.udg.mx

[2] Tecnológico Nacional de México/Instituto Tecnológico de Tepic, Av. Tecnológico 2595, Lagos del Country, Tepic 63175, Mexico; jsanchezb@ittepic.edu.mx (J.A.S.-B.); vzamora@ittepic.edu.mx (V.Z.-G.)

* Correspondence: alarios@cualtos.udg.mx

Abstract: An effective way to obtain the optimal parameters of a process or experiment is the response surface method. Using the Box–Behnken design further decreases the number of experiments needed to obtain sufficient data to obtain a reliable equation. From the equation, it is possible to predict the behavior of the response with respect to the combination of variables involved. In this study we evaluated the photocatalytic activity of the synthesized TiO₂ for the degradation of acetaminophen, a frequently used and uncontrolled drug that has been detected with increasing frequency in wastewater effluents. The variables used for this study were pH, contaminant concentration (acetaminophen) and catalyst dose. We found, with a 95% confidence level, that 99% of the contaminant can be degraded to pH 10, contaminant to 35 mg/L and a catalyst dose of 0.15 g TiO₂.

1. Introduction

The response surface method (RSM) is one of the experimental statistical design techniques that is applied to building models and investigating the effects and interactions of all selected operating conditions on the response of a given experiment [1,2]. This method is very effective for the optimization of complex processes, and allows researchers to obtain the optimal conditions of an operation [3]; this results in more convenience, in that it saves time, labor and costs [4,5]. Among the most important RSM methodologies, are the 2^k and 3^k factorial designs, where 2 and 3 are the number of levels to test, and *k* is the number of controllable factors [3]. However, a full factorial design (FFD) is impractical because of the large number of experiments required to predict the outcome [6]. Due to the above, in a statistical design, what is sought is to accurately predict all the positions of the factorial space that are equidistant from the center [6]–the most common being Artificial Neural Networks (ANN), the Central Composite Design (CCD) and the Box–Benkhen Design (BBD)–n order to optimize the response. The Box–Behnken Design (BBD) provides us with a second-order response model and can maximize the amount of complex information with minimum experimentation time [7,8]; even more importantly, it can avoid the need for analyses of their extreme combinations. With this technique, it is possible to investigate the effects from three to seven factors, each of them with three levels of experimental condition (level: low, medium and high). This is proven to be more efficient than other response surface designs [2,9]. The data obtained from the BBD have been evaluated using the analysis of variance (ANOVA) technique, to determine which of the controllable factors are statistically significant, since it compares the quadratic sum of the sources of variation and provides a confidence interval above 90% [3,6,9]. Among the most investigated variables in photocatalysis in an RSM are the dose of the catalyst, the concentration of the contaminant and the pH of the solution [2,5,8–10]. On a smaller scale, the following have been studied:

the wavelength of the irradiation source [11], the dose of O_2 [10], and the size of the TiO_2 particles [6].

Titanium dioxide (TiO_2) has been a subject of study in recent decades due to its wide range of applications in areas such as pigments [12], lubricants [7], optical sensors [13], food and cosmetics [14], either in thin films as two-dimensional material [15], or in nanoparticles—as well as nanocomposites of TiO_2-Fe_2O_3 [16], Ti-Zr [17] and graphene-TiO_2 [18]—for photocatalytic applications in hydrogen production [19,20], and water treatment [21]. In this sense, the elimination of mainly phenolic compounds [6], organic pollutants [10], colorants [2,22], pesticides and herbicides [23,24], and drugs [3,8,25–27] has been studied. In addition, its ability to be used for prolonged periods of time and the reproducibility of the results of photocatalytic activity have been studied [19,26]. The photocatalytic process is an advanced oxidation method based on the generation of hydroxyl radicals, when UV light is irradiated on a semiconductor catalyst [2]. When TiO_2 nanoparticles are exposed to a light source that has an energy higher than its bandgap (TiO_2 = 3.2 eV), it produces the most powerful intermediate oxidative radicals [10]. Irradiation causes electrons in the valence band to migrate to the conduction band, creating the electron-hole pair ($e^- - h^+$) [14]. On the surface of TiO_2, the holes (h^+) of the valence band can react with hydroxide ions (OH) or adsorbed H_2O; therefore, the adsorption properties of the substrate affect the reaction rate [5,6]. Meanwhile, the electrons (e^-) of the conduction band can be captured or interact with oxygen molecules; therefore, the availability of oxygen in the aqueous phase has an effect on the photocatalytic activity to generate hydroxyl radicals [20]. Due to their high oxidation potential, they react with most organic compounds to form simpler species such as CO_2 and H_2O, achieving mineralization [3]. On the other hand, statistical methods have been reported to investigate the effects of catalyst dose, pH, contaminant concentration, light source wavelength, etc., albeit studying one parameter at a time [22,23]. However, these methods are inefficient to estimate the effects between the interaction of the factors, so a reliable prediction cannot be made in a photocatalytic system [9,28].

In this work, the efficiency of the photocatalytic degradation of acetaminophen with TiO_2 is investigated, using the analysis of the influence of three factors and their interactions on the determination of the optimal conditions of the experiment. The factors to be studied are catalyst dose, reaction pH and contaminant concentration, using a BBD as an RSM optimization method.

2. Materials and Methods

2.1. Chemical Reagents

Ethyl alcohol (Aldrich 99.4%), distilled H_2O and titanium (IV) butoxide ($C_{16}H_{36}O_4Ti$, Sigma-Aldrich 97%) were used as precursors.

2.2. Synthesis of TiO_2

TiO_2 was synthesized by the sol-gel method. Ethyl alcohol and H_2O with a molar ratio of 8:1 were placed in a three-necked flask, and the solution was heated to 70 °C to add titanium butoxide dropwise. After 24 h, the material was dried at 100 °C and ground in an agate mortar. Finally, the material was calcined at 500 °C for 5 h with a heating ramp of 2 °C/min.

2.3. Characterization of TiO_2

For the micrographs, a TESCAN brand scanning electron microscope, model MIRA3 (LMU, London, UK), with a power of 20.0 KV, was used.

X-ray diffraction studies were performed in Panalytical equipment, empyrean model (Empyrean, Almelo, The Netherland), with Cu Kα radiation (λ = 0.154 nm) and with a diffraction angle (2θ) of 10 to 90°, using a step of 0.03° and a time of 3 s per step.

UV-vis diffuse reflectance spectra were obtained with a Shimadzu UV-Vis spectrophotometer, model UV-2600 (Shimadzu UV-2600, Tokyo, Japan) coupled with an integrating

sphere for diffuse reflectance studies. The diffuse reflectance spectrum was obtained and transformed to a magnitude proportional to the extinction coefficient (α) through the Kubelka–Munk function, using wavelengths in the range of 900 to 190 nm.

X-ray photoelectron spectroscopy was analyzed in SPECS model III equipment (Thermo Scientific K Alpha, Tokyo, Japan), with monochromatic Al K radiation (1486 eV) and a scanning resolution of 0.1 eV. The survey and high-resolution spectra of the sample were recorded in a constant step energy mode at 60 eV, using a spot size of 400 mm. The vacuum in the analysis chamber was maintained at 1×10^{-9} Torr during the analysis. Sample loading effects were corrected for using the O1s offset from 531.0 eV. The system was calibrated by determining the position of the Au 4f peak at 84.00 ± 0.05 eV.

2.4. Photocatalytic Activity of TiO$_2$

The photocatalytic activity of TiO$_2$ for the degradation of acetaminophen (ACTP) was investigated using a 400 mL pyrex reactor under UV light, where a 1 mW cm^{-2} UV lamp with a wavelength of 256 nm was placed, covered with a quartz tube for immersion. 350 mL of aqueous solution was prepared for each reactor, according to the experimental design developed, to evaluate the variables of contaminant concentration (20, 30 and 40 mg L^{-1}), pH (4, 7 and 10) and catalyst dose (50, 100 and 150 mg) under constant stirring. Before proceeding to the photoactivity test, the solution was kept in a dark environment to create an adsorption–desorption equilibrium [29]. The samples were analyzed in a Shimadzu 2600 model UV-Vis spectrophotometer (Shimadzu UV-2600, Tokyo, Japan), from 500 to 190 nm. The degradation curves were obtained by measuring the absorbance at the wavelength (243–246 nm) corresponding to acetaminophen [11,27], as a function of time (every 30 min for 3 h). To calculate the percentage efficiency of acetaminophen degradation, Equation (1) was used:

$$\text{Yield (\%)} = \frac{C_A - C_t}{C_A} * 100 \tag{1}$$

where C_A is the initial concentration of the contaminant and C_t is the final concentration of the contaminant.

The total organic carbon of the samples was analyzed using the Shimadzu model TOC-LCSN equipment (Shimadzu, Tokyo, Japan), and applying Equation (2)

$$\text{TOC} = \text{TC} - \text{IC}, \tag{2}$$

where TOC is the amount of total organic carbon (mg L^{-1}), TC is the total amount of carbon (mg L^{-1}), and IC is the amount of inorganic carbon (mg L^{-1}) present in the aqueous solution.

To calculate the percentage yield of TOC conversion, the Equation (3) was used:

$$\text{Yield (\%)} = \frac{\text{TOC}_0 - \text{TOC}_{\text{residual}}}{\text{TOC}_0} * 100 \tag{3}$$

where TOC$_0$ is the initial concentration and TOC$_{\text{residual}}$ is the final concentration.

2.5. Response Surface Method (RSM)

The RSM establishes a mathematical relationship between the variables evaluated and the results obtained to adapt a second-order polynomial model according to Equation (4):

$$y = \beta_0 + \sum_{i=1}^{k} \beta_i x_i + \sum_{i=1}^{k} \beta_{ii} x_i^2 + \sum_{i=1}^{k} \sum_{j=i+j}^{k} \beta_{ij} x_i x_j + \varepsilon \tag{4}$$

where y is the response variable, x_i is the value for the parameters X$_A$, X$_D$ and X$_{\text{pH}}$, β_0 is a constant, β_i is the value of the regression coefficient, k is the number of independent variables and ε is the effect of the experimental error.

For the statistical analysis, the analysis of variance method (ANOVA) was applied, establishing the probability value (p) of 95% ($p < 0.05$), as the statistical significance level

parameter for the proposed model. On the other hand, the efficiency of the model was evaluated by means of the correlation coefficient (R^2) and the adjusted correlation coefficient (R^2 adjusted) and the reproducibility was determined by the experimental error.

Data were expressed as mean standard deviation (n). The analyzes of variance used to assess whether a term has a significant effect ($p < 0.05$) were performed using one-factor ANOVA and the Tukey test, both analyzed using the STATISTICA v software. 10 (Statsoft, Tulsa, OK, USA).

To determine the optimal conditions for degradation and mineralization of acetaminophen in a photocatalytic reactor, the 3-factor Box–Benkhen design with 3 central points and 3 repetitions was applied to determine the optimal conditions to maximize degradation efficiency of the acetaminophen contaminant. The method consisted of defining a minimum or low level (denoted as −1), a central or medium level (denoted as 0), and a high or maximum level (denoted as 1) for each experimental factor, as shown in Table 1. The effects of the interactions between the experimental factors and their influence on the response were quantified to optimize: the initial concentration of the acetaminophen contaminant (X_A mg L^{-1}), the dose of the catalyst (X_D mg) and the pH of the solution (X_{pH} pH).

Table 1. Variables and levels established for statistical analysis.

Variables	Factor	Range and Established Levels		
		−1	**0**	**1**
X_A	ACTP concentration [1]	20	30	40
X_D	Catalyst dosageTiO$_2$ [2]	50	100	150
X_{pH}	pH of solution	4	7	10

[1] mg∗L^{-1}, [2] mg.

Experimental factors and levels were selected for each factor based on literature values, available resources and results of preliminary experiments.

3. Results and Discussion

3.1. Characterization

3.1.1. Scanning Electron Microscopy (SEM)

In Figure 1, the micrographs of TiO$_2$ SEM, which presents irregularly shaped hemispherical agglomerated morphology, can be seen. It is suggested that this type of agglomeration is due to electrostatic attractions and/or ionization energy [9].
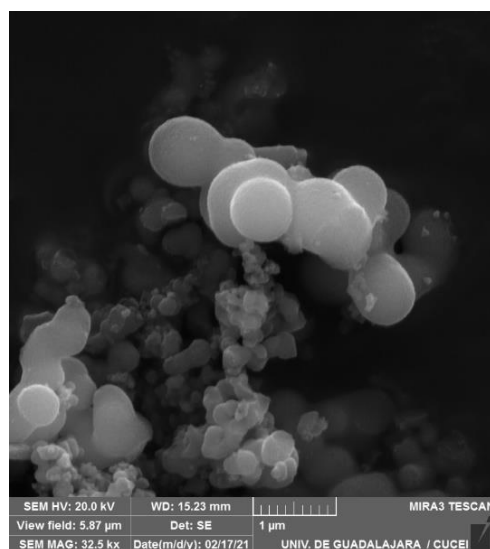

Figure 1. Micrograph of the TiO$_2$ NPs.

3.1.2. X-ray Diffraction (XRD)

Figure 2 shows the XRD patterns of the sample (calcination at 500 °C). The TiO_2 pattern is consistent with diffractions at 2θ = 25.4°, 36°, 46°, 53, 53°, 65°, which are assigned to the anatase crystal phase (JCPDD: 21 1272) and correspond to index Miller (101), (004), (200), (105), (211) and (204). This is corroborated with previous studies where the anatase phase is obtained after anneal at 500 °C [17,30]. It also suggests that the bonds of the original structure are maintained after calcination.
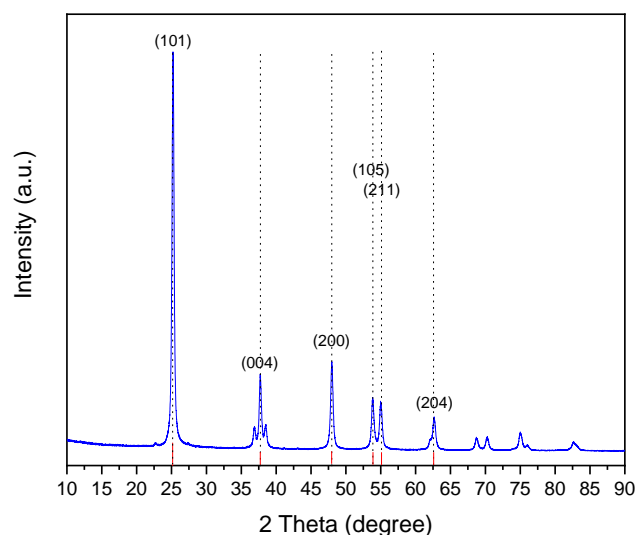

Figure 2. X-ray diffractogram of TiO_2.

3.1.3. UV-Vis Spectroscopy

Figure 3 shows the UV-Vis spectrum of TiO_2 as a photocatalyst. The spectrum shows an important absorption within the UV range (<400 nm), where two peaks are shown in the region from 400 to 190 nm; this suggests that the peak at 210 nm (green line) could be associated with charge transfer of the ligand–metal between the tetrahedral Ti^{4+} and an an oxygenated ligand such as O^{2-}, and the second peak at 350 nm (red line) is attributed to the Ti^{4+} cations in the octahedral environment, as well as to the anatase phase [5]. On the other hand, the calculated E_g value was 3.20 eV (Figure 4), which coincides with those reported in the literature [31].
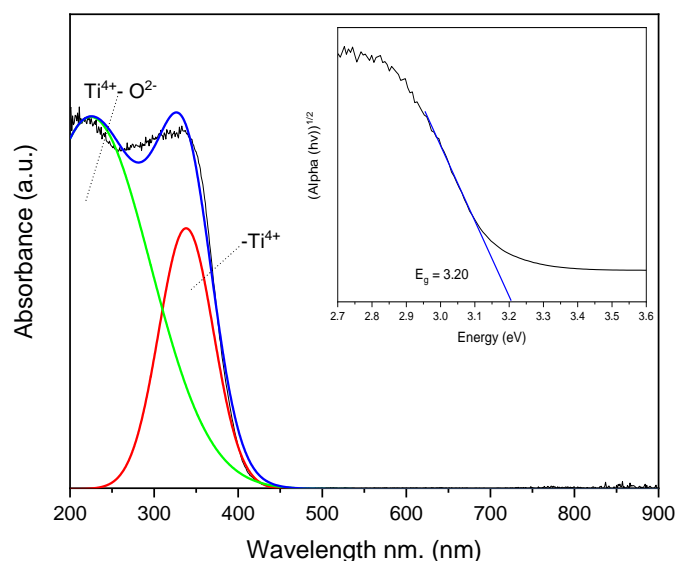

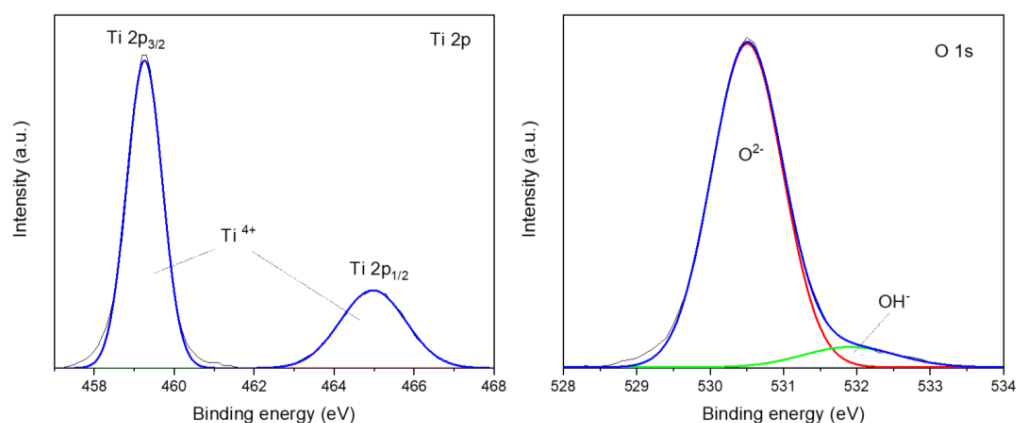**Figure 3.** UV−Vis spectrum of TiO_2.

Figure 4. XPS spectra of TiO_2.

3.1.4. X-ray Photoelectron Spectroscopy

The superficial chemical composition of TiO_2 was analyzed by X-ray photoelectron spectroscopy. Figure 4 shows the spectra for Ti 2p, O1s and C1s. In Figure 4 (Ti 2p), the components of the split spin-orbit of Ti 2p, related to the components Ti $2p_{1/2}$ and Ti $2p_{3/2}$, can be seen; these are found in the band position of 455 and 468 eV, respectively; these peaks are associated with the presence of Ti^{4+} species, suggesting that there are no defects associated with the TiO_2 lattice. On the other hand, the behavior of oxygen (O1s), is characteristic of the material located at 530.5 eV, where oxygen tends to attract electrons, making the nucleus more electronegative [17]. Furthermore, the bands located at 532 eV, are attributable to the presence of weakly adsorbed species associated with surface hydroxyl (OH) groups (Figure 4 (O 1s)) [30].

3.2. Photocatalytic Activity

3.2.1. Model Validation

For the response surface optimization study, the photocatalytic degradation of acetaminophen was performed at each design point of the three factors (catalyst weight, contaminant concentration, and pH solution) at three levels each. Considering this design, three replicates of 37 experiments were performed.

In order to avoid any systematic bias in the results, the experiments were performed randomly and the responses of other process factors, not selected for the object of study of the experimental design, are considered an error for the experimental design. The coefficients of the quadratic model, which describes the percentage of degradation (efficiency) as a function of the reaction condition (independent variable), were calculated by means of a multiple regression analysis on the experimental data.

The analysis of the BBD was carried out considering a quadratic model for its prediction. The results of the coefficients obtained from the effect of the following factors are presented individually in Table 2, in addition to the linear (L) and quadratic (Q) interactions of the model: X_A—concentration of acetaminophen (ACTP); X_{pH}—pH; and X_D—dose of catalyst (Wt of catalyst). Those factors and interactions that present a significant effect ($p < 0.05$) are shown, and are that of the ACTP factor that had the greatest effect (linear and quadratic coefficient, respectively), followed by the linear coefficient of the pH factor, the linear coefficient of the "Wt of catalyst" factor, and the interaction of the linear coefficient of the ACTP and pH factors. The obtained model has an R^2 fit of 0.85 and R^2 adjusted of 0.81, for which the model is considered to have a good prediction.

Table 2. Effect estimates for the efficiency quadratic model.

Factor	Effect	Std.Err.	t (27)	p
Mean/Interc.	87.117	0.977	89.178	0.000
(1) [ACTP] (L)	−20.361	2.398	−8.492	0.000
[ACTP] (Q)	11.037	1.718	6.423	0.000
(2) pH (L)	12.128	2.41	5.032	0.000
pH (Q)	3.03	1.727	1.755	0.091
(3) Wt of catalyst (L)	4.934	2.346	2.103	0.045
Wt of catalyst (Q)	−0.309	1.718	−0.18	0.859
1L by 2L	16.57	3.481	4.761	0.000
1L by 3L	4.832	3.334	1.449	0.159
2L by 3L	−1.133	3.3	−0.343	0.734

According to the mathematical model, the optimal conditions of the process are those presented in Table 3. It is observed that the optimal conditions are an ACTP level of 35, with a pH of 10 and Wt of catalyst of 150 mg. Table 4 shows the prediction under optimal conditions, breaking down the values that would be obtained in the model coefficients and that would allow an efficiency value of 99.03%.

Table 3. Optimal process conditions.

Factor	Level Factor	Predicted Efficiency	Desirability Value	−95% CI Efficiency	+95% CI Efficiency
ACTP concentration [1]	35	99.034	1.000	93.062	105.006
Catalyst dosageTiO$_2$ [2]	150				
pH of solution	10				

[1] mg$*$L^{-1}, [2] mg.

Table 4. Breakdown of model coefficients under optimal conditions.

Factor	Regression Coefficients	Value	Value
Constant	63.005	0	0
(1) [ACTP] (L)	3.188	35	111.569
[ACTP] (Q)	−0.11	1225	−135.202
(2) pH (L)	−1.174	10	−11.736
pH (Q)	−0.337	100	−33.662
(3) Wt of catalyst (L)	−0.094	150	−14.084
Wt of catalyst (Q)	0	22,500	2.781
1L by 2L	0.276	350	96.661
1L by 3L	0.005	5250	25.366
2L by 3L	−0.004	1500	−5.664
Predicted			99.034
−95% Conf.			93.062
+95% Conf.			105.006

Acetaminophen concentration (ACTP); Catalyst dosage TiO$_2$ (Wt of catalyst); pH of solution (pH).

The t-value of effects is set on the Pareto chart (Figure 5). The Pareto diagram was obtained to observe the hierarchy of the effects in each term on the efficiency. If the t-value of effects set on the Pareto charts is less than or equal to the significance level ($p < 0.05$), this reveals that there is a statistically significant association between the response variable and the term in the model. Significant effects on efficiency were found in the following order: ACTP Linear > ACTP Quadratic > pH Linear > ACTP Linear * pH Linear > Wt of Catalyst Linear. The regression coefficients of the quadratic model (Equation (5) and Table 4) show the effects of each term on the efficiency. Positive coefficients indicated an increase in efficiency, while negative coefficients indicated a decrease in efficiency. In this sense, it was observed that ACTP Linear and ACTP Linear * pH Linear favored greater efficiency. However, the quadratic ACTP, linear pH and quadratic Wt of catalyst terms

decreased the efficiency, and the other terms in the model were not statistically significant ($p > 0.05$); therefore, they do not influence efficiency.
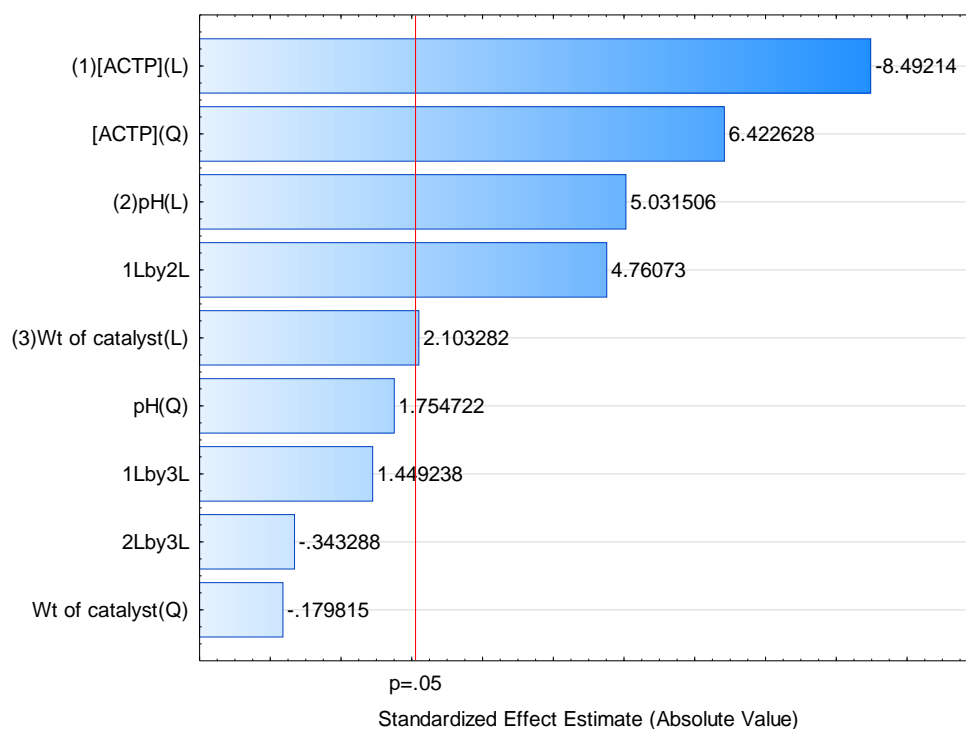

Figure 5. Pareto chart.

Corresponding to the experimental dates, the general mathematical model is the one presented in Equation (5):

$$
\begin{aligned}
\text{Efficiency} = \quad & 63.00 + 3.18 * \text{ACTP} - 0.11 * \text{ACTP}^2 - 1.17 * \text{pH} - 0.33 * \text{pH}^2 \\
& -0.09\text{Wt of Catalyst} + 0.00 * \text{Wt of Catalyst}^2 + 0.27 * \text{ACTP} \\
& *\text{pH} + 0.00 * \text{ACTP} * \text{Wt of Catalyst} - 0.00 * \text{pH} \\
& *\text{Wt of Catalyst}
\end{aligned}
\tag{5}
$$

This model describes the regression coefficients (Table 4, column of regression coefficients), corresponding to the quadratic and linear parts of the equation as a function of the factors (ACTP, pH, Wt of catalyst) and their interactions, with which the behavior of the response variable (efficiency) can be predicted.

In Figure 6a, the relationship between the pH and ACTP response surface is presented; when the Wt of Catalyst value is set to 100, there is an efficiency increase with a decrease in ACTP concentration, but it remains stable throughout the basic pH. In Figure 6b, the response surface graph of Wt of Catalyst and ACTP at pH 7.24 is shown; it can be noted that higher efficiency can be obtained when Wt of Catalyst increases, depending on the increase in the initial ACTP concentration. On the other hand, Figure 6c shows the response surface plot of pH and Wt of Catalyst at a fixed ACTP value of 29.72. It can be seen that the highest efficiency values are found in pH values from 8 to 11, and at any Wt of Catalyst; however, due to process conditions, the appropriate pH is 10. In addition, the initial ACTP concentration also has an effect, with an optimized dose of 35 mg/L for maximum degradation efficiency.

(**a**)
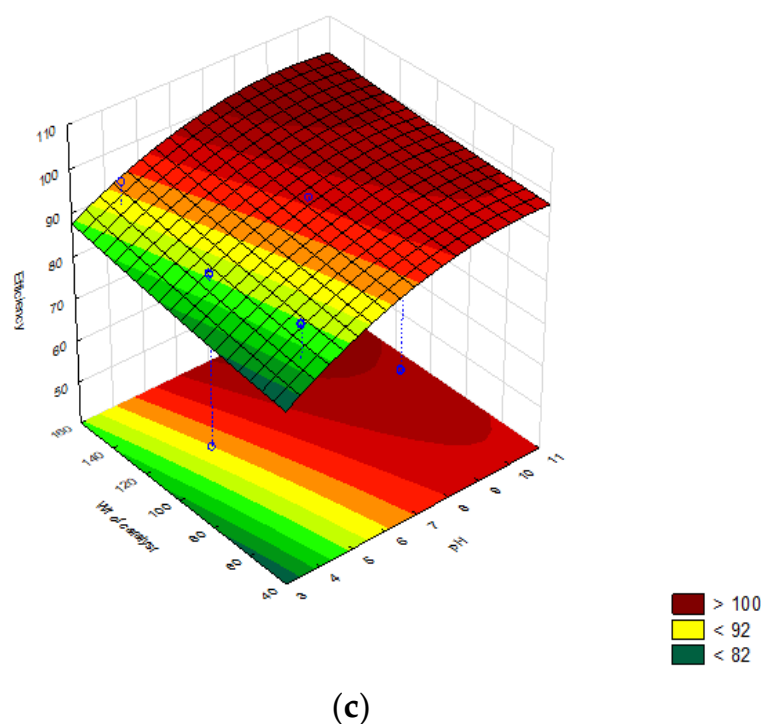

(**b**)

Figure 6. *Cont.*

(c)
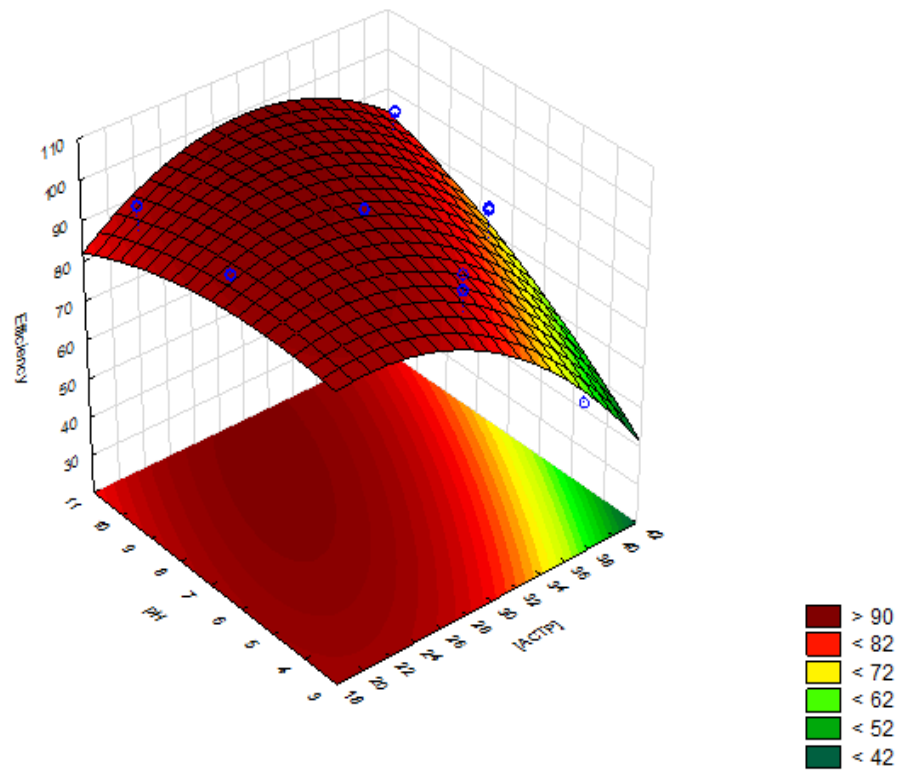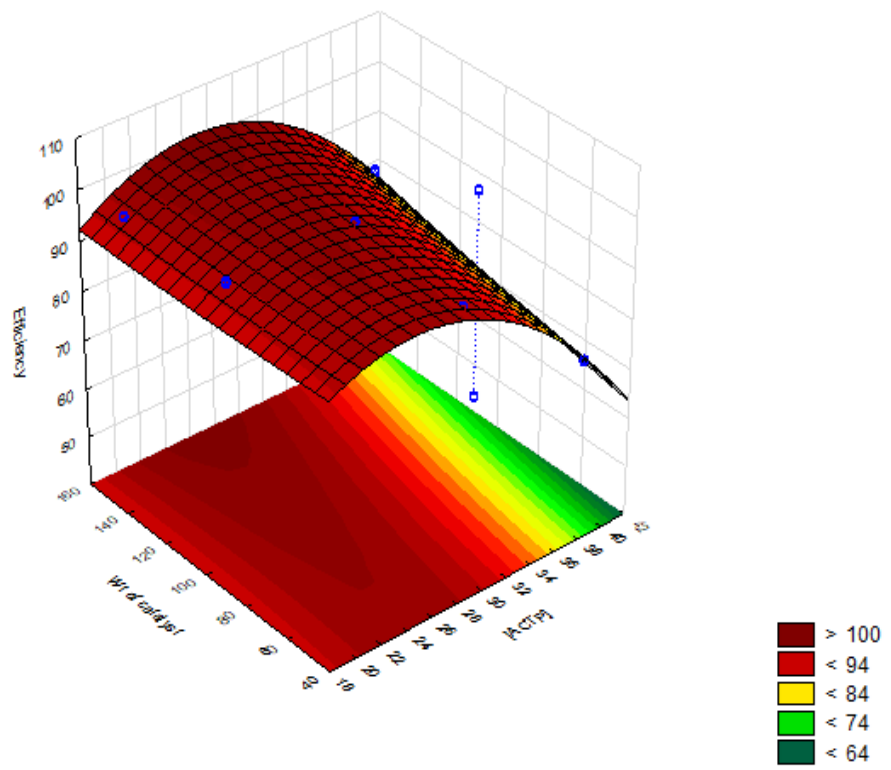
Figure 6. Response surface plot of: (**a**) pH and ACTP at a fixed Wt of Catalyst value of 100; (**b**) Wt of Catalyst and ACTP at a fixed pH value of 7.24; and (**c**) pH and Wt of Catalyst at a fixed ACTP value of 29.72.
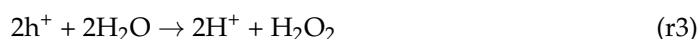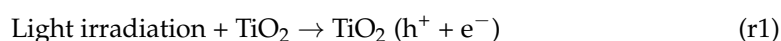
Additional experiments were performed to confirm the validity and accuracy of the response surface model within the design variables considered. It was compared with the degradation percentage calculated using experimental data at a 0.15 g TiO_2 dose, a 35 mg/L contaminant concentration and 10 pH in the solution, obtaining a degradation percentage of 97.19%, with an S.D. of 0.04%. The experimental response is 1.86% lower than the expected maximum response.

3.2.2. TOC Analysis

Furthermore, in the additional experiments, the samples used for the TOC analysis were also obtained. The percentage of mineralization was obtained using Equation (3), obtaining 60% during the first 3 h of irradiation and continuing up to 95% at 6 h of irradiation.

3.2.3. Proposed Photocatalytic Mechanism

TiO_2 is capable of absorbing photons from UV-light-generating holes (h^+) in the valence band and e^- in the conduction band, as shown in reaction 1 (r1). Those h^+ can then form hydroxyl radicals ($OH^\bullet$) through oxidative reactions 2 to 4 ((r2) to (r4)).

$$\text{Light irradiation} + TiO_2 \rightarrow TiO_2\,(h^+ + e^-) \tag{r1}$$

$$h^+ + H_2O \rightarrow H^+ + OH^\bullet \tag{r2}$$

$$2h^+ + 2H_2O \rightarrow 2H^+ + H_2O_2 \tag{r3}$$

$$H_2O_2 \rightarrow OH^\bullet + OH^\bullet \tag{r4}$$

Furthermore, the electrons in the conduction band form super oxide radical anions ($O_2^{\bullet-}$) via reductive reactions, as shown in the follow reactions 5 to 7 ((r5) to (r7))

$$2e^- + O_2 \rightarrow O_2^{\bullet-} \tag{r5}$$

$$O_2^{\bullet-} + 2H^+ \rightarrow H_2O_2 + O_2 \tag{r6}$$

$$H_2O_2 \rightarrow OH^\bullet + OH^\bullet \tag{r7}$$

Radicals $O_2^{\bullet-}$ and $OH^\bullet$ are strong oxidants that can oxidize recalcitrant compounds such as acetaminophen, because $OH^\bullet$ tends to remove hydrogen or attack the C-C unsaturated bonds, and the $O_2^{\bullet-}$ can lead to total mineralization [5].

4. Conclusions

TiO$_2$ was successfully prepared by the sol-gel method. The TiO$_2$ nanoparticles possess a spherical agglomeration in cylindrical form. The photocatalyst band gap energy is 3.2 eV and exhibits photocatalytic activity in the degradation of ACTP under UV-Vis light irradiation. The regression coefficients of the equation obtained show the effects of each variable and their interactions on the efficiency response of our degradation experiments. A catalyst loading of 0.15 g is the optimum dosage to enhance the removal rate. The amount of ACTP removed increases with the initial concentration of the photocatalyst. Increasing the pH value does not improve removal efficiency due to the surface charge. A multivariate experimental design was used to develop a quadratic model as the functional relationship between the percentage removal of ACTP and the three independent variables. Response surface methodology with a BBD was successfully employed to investigate the significance of the factors at different levels during the ACTP removal. A satisfactory goodness-of-fit was observed between the predictive and experimental results. This indicates that response surface methodology is applicable in optimization of the removal of ACTP by TiO$_2$.

References

1. Hafeez, A.; Taqvi, S.A.A.; Fazal, T.; Javed, F.; Khan, Z.; Amjad, U.S.; Bokhari, A.; Shehzad, N.; Rashid, N.; Rehman, S.; et al. Optimization on cleaner intensification of ozone production using Artificial Neural Network and Response Surface Methodology: Parametric and comparative study. *J. Clean. Prod.* **2020**, *252*, 119833. [CrossRef]
2. Mortazavian, S.; Saber, A.; James, D.E. Optimization of Photocatalytic Degradation of Acid Blue 113 and Acid Red 88 Textile Dyes in a UV-C/TiO$_2$ Suspension System: Application of Response Surface Methodology (RSM). *Catalysts* **2019**, *9*, 360. [CrossRef]
3. Vebber, M.C.; da Silva Crespo, J.; Giovanela, M. Self-assembled thin films of PAA/PAH/TiO$_2$ for the photooxidation of ibuprofen. Part I: Optimization of photoactivity using design of experiments and surface response methodology. *Chem. Eng. J.* **2019**, *360*, 1447–1458. [CrossRef]
4. Peng, T.; Ray, S.; Veeravalli, S.S.; Lalman, J.A.; Arefi-Khonsari, F. The role of hydrothermal conditions in determining 1D TiO$_2$ nanomaterials bandgap energies and crystal phases. *Mater. Res. Bull.* **2018**, *105*, 104–113. [CrossRef]
5. Chaker, H.; Ameur, N.; Saidi-Bendahou, K.; Djennas, M.; Fourmentin, S. Modeling and Box-Behnken design optimization of photocatalytic parameters for efficient removal of dye by lanthanum-doped mesoporous TiO$_2$. *J. Environ. Chem. Eng.* **2021**, *9*, 104584. [CrossRef]
6. Ray, S.; Lalman, J.A.; Biswas, N. Using the Box-Benkhen technique to statistically model phenol photocatalytic degradation by titanium dioxide nanoparticles. *Chem. Eng. J.* **2009**, *150*, 15–24. [CrossRef]
7. Mohamad, N.S.; Kasolang, S. Optimized characterization of response surface methodology on lubricant with titanium oxide nanoparticles. *Ind. Lubr. Tribol.* **2017**, *69*, 387–392. [CrossRef]

8. Li, L.; Ma, Q.; Wang, S.; Song, S.; Li, B.; Guo, R.; Cheng, X.; Cheng, Q. Photocatalytic performance and degradation mechanism of aspirin by TiO$_2$ through response surface methodology. *Catalysts* **2018**, *8*, 118. [CrossRef]

9. KC, C.; Prabhu, T.N.; Kiran, R.R.S.; Krishna, R.H. Applications of artificial neural network and Box-Behnken Design for modelling malachite green dye degradation from textile effluents using TiO$_2$ photocatalyst. *Environ. Eng. Res.* **2021**, *27*, 200553. [CrossRef]

10. Tetteh, E.K.; Rathilal, S.; Naidoo, D.B. Photocatalytic degradation of oily waste and phenol from a local South Africa oil refinery wastewater using response methodology. *Sci. Rep.* **2020**, *10*, 8850. [CrossRef]

11. Yap, H.C.; Pang, Y.L.; Lim, S.; Lai, C.W.; Abdullah, A.Z. Enhanced sonophotocatalytic degradation of paracetamol in the presence of Fe-doped TiO$_2$ nanoparticles and H$_2$O$_2$. *Environ. Earth Sci.* **2020**, *79*, 457. [CrossRef]

12. Sun, S.; Ding, H.; Hou, X. Preparation of CaCO$_3$-TiO$_2$ composite particles and their pigment properties. *Materials* **2018**, *11*, 1131. [CrossRef] [PubMed]

13. Kim, W.T.; Choi, W.Y. Fabrication of TiO$_2$ photonic crystal by anodic oxidation and their optical sensing properties. *Sens. Actuators A Phys.* **2017**, *260*, 178–184. [CrossRef]

14. Musial, J.; Krakowiak, R.; Mlynarczyk, D.T.; Goslinski, T.; Stanisz, B.J. Titanium dioxide nanoparticles in food and personal care products—What do we know about their safety? *Nanomaterials* **2020**, *10*, 1110. [CrossRef]

15. Tareen, A.K.; Khan, K.; Aslam, M.; Liu, X.; Zhang, H. Confinement in two-dimensional materials: Major advances and challenges in the emerging renewable energy conversion and other applications. *Prog. Solid State Chem.* **2021**, *61*, 100294. [CrossRef]

16. Ameur, N.; Bachir, R.; Bedrane, S.; Choukchou-Braham, A. A Green Route to Produce Adipic Acid on TiO$_2$–Fe$_2$O$_3$ Nanocomposites. *J. Chin. Chem. Soc.* **2017**, *64*, 1096–1103. [CrossRef]

17. Pérez-Larios, A.; Rico, J.L.; Anaya-Esparza, L.M.; Vargas, O.A.G.; González-Silva, N.; Gómez, R. Hydrogen production from aqueous methanol solutions using Ti–Zr mixed oxides as photocatalysts under UV irradiation. *Catalysts* **2019**, *9*, 938. [CrossRef]

18. Lin, L.; Wang, H.; Xu, P. Immobilized TiO2-reduced graphene oxide nanocomposites on optical fibers as high performance photocatalysts for degradation of pharmaceuticals. *Chem. Eng. J.* **2017**, *310*, 389–398. [CrossRef]

19. Li, F.; Huang, Y.; Peng, H.; Cao, Y.; Niu, Y. Preparation and Photocatalytic Water Splitting Hydrogen Production of Titanium Dioxide Nanosheets. *Int. J. Photoenergy* **2020**, *2020*, 3617312. [CrossRef]

20. Eidsvåg, H.; Bentouba, S.; Vajeeston, P.; Yohi, S.; Velauthapillai, D. TiO$_2$ as a photocatalyst for water splitting—An experimental and theoretical review. *Molecules* **2021**, *26*, 1687. [CrossRef]

21. Abel, S.; Jule, L.T.; Belay, F.; Shanmugam, R.; Dwarampudi, L.P.; Nagaprasad, N.; Krishnaraj, R. Application of Titanium Dioxide Nanoparticles Synthesized by Sol-Gel Methods in Wastewater Treatment. *J. Nanomater.* **2021**, *2021*, 3039761. [CrossRef]

22. Lee, J.; Seong, S.; Jin, S.; Jeong, Y.; Noh, J. Synergetic photocatalytic-activity enhancement of lanthanum doped TiO$_2$ on halloysite nanocomposites for degradation of organic dye. *J. Ind. Eng. Chem.* **2021**, *100*, 126–133. [CrossRef]

23. Rao, T.N.; Hussain, I.; Anwar, M.S.; Koo, H. Photocatalytic degradation kinetics of pesticide residues in different pH waters using metal-doped metal oxide nanoparticles. *EQA Int. J. Environ. Qual.* **2020**, *36*, 37–44. [CrossRef]

24. Martínez, C.P.C.; Ortega, I.A.A.; Sarmiento, H.A.R.; Morales, F.J.T.; Romero, J.R.G. Photocatalytic degradation of the 2,4-dichlorophenoxyacetic acid herbicide using supported iridium materials. *Cienc. Desarro.* **2021**, *12*, 125–134. [CrossRef]

25. da Cunha, R.; do Carmo Batista, W.V.F.; de Oliveira, H.L.; dos Santos, A.C.; dos Reis, P.M.; Borges, K.B.; Martelli, P.B.; Furtado, C.A.; de Fátima Gorgulho, H. Carbon Xerogel/TiO$_2$ composites as photocatalysts for acetaminophen degradation. *J. Photochem. Photobiol. A Chem.* **2021**, *412*, 113248. [CrossRef]

26. Jallouli, N.; Elghniji, K.; Trabelsi, H.; Ksibi, M. Photocatalytic degradation of paracetamol on TiO$_2$ nanoparticles and TiO$_2$/cellulosic fiber under UV and sunlight irradiation. *Arab. J. Chem.* **2017**, *10*, S3640–S3645. [CrossRef]

27. Rimoldi, L.; Meroni, D.; Falletta, E.; Ferretti, A.M.; Gervasini, A.; Cappelletti, G.; Ardizzone, S. The role played by different TiO$_2$ features on the photocatalytic degradation of paracetamol. *Appl. Surf. Sci.* **2017**, *424*, 198–205. [CrossRef]

28. Inger, M.; Dobrzyńska-Inger, A.; Rajewski, J.; Wilk, M. Optimization of ammonia oxidation using response surface methodology. *Catalysts* **2019**, *9*, 249. [CrossRef]

29. Hegyi, A.; Szilagyi, H.; Grebenișan, E.; Sandu, A.V.; Lăzărescu, A.-V.; Romila, C. Influence of TiO$_2$ Nanoparticles Addition on the Hydrophilicity of Cementitious Composites Surfaces. *Appl. Sci.* **2020**, *10*, 4501. [CrossRef]

30. Pérez-Larios, A.; Torres-Ramos, I.; Zanella, R.; Rico, J.L. Ti-Co mixed oxide as photocatalysts in the generation of hydrogen from water. *Int. J. Chem. React. Eng.* **2022**, *20*, 129–140. [CrossRef]

31. Li, S.; Yang, Y.; Su, Q.; Liu, X.; Zhao, H.; Zhao, Z.; Li, J.; Jin, C. Synthesis and photocatalytic activity of transition metal and rare earth element co-doped TiO$_2$ nano particles. *Mater. Lett.* **2019**, *252*, 123–125. [CrossRef]